Influence of the Catalyst Hydrogen Pretreatment on the Growth of Vertically Aligned Nitrogen-Doped Carbon Nanotubes

P. Ayala,*[,†,‡] A. Grüneis,[†] T. Gemming,[†] B. Büchner,[†] M. H. Rümmeli,[†,§] D. Grimm,[†] J. Schumann,[†] R. Kaltofen,[†] F. L. Freire Jr.,[‡] H. D. Fonseca Filho,[‡] and T. Pichler[†]

Leibniz Institute for Solid State and Materials Research Dresden, P.O. Box 270116, D-01171 Dresden, Germany, Departamento de Fisica, Pontifícia Universidade Católica do Rio de Janeiro, 22453-900 Rio de Janeiro, Brazil, and Institute of Chemical and Environmental Engineering, Szczecin University of Technology, 70-322 Szczecin, Poland

Received June 11, 2007. Revised Manuscript Received September 18, 2007

Thin vertically aligned N-doped nanotubes with narrow layered nanotube diameter distribution and a defined doping level have been synthesized by chemical vapor deposition. Multilayered catalysts and a pure acetonitrile C/N feedstock have been employed. The observed nitrogen content was up to 6% with a predominant sp^2 bonding configuration in relation to other nitrogen incorporated forms. Depending on the process parameters, we were able to tune the nitrogen content and the formation ratio of small nanotubes to bamboo nanotubes. The use of multilayer catalyst allows a large temperature window in which substitutionally doped structures form in comparison to other catalysts.

1. Introduction

The outstanding properties encountered in carbon nanotubes make these nanometer-sized structures a very active and attractive field of research.[1] In particular, single- and double-walled tubes might successfully be used in applications in the semiconductor technology when their electronic properties are tuned in a controlled manner. An ideal alternative is the presence of substitutional doping atoms such as N or B introduced in the hexagonal lattice, leading to the formation of n or p type semiconductors.[2]

Regarding the synthesis of N-doped nanotubes, common nanotube growth methods such as arc-discharge[3,4] and chemical vapor deposition (CVD) related methods,[5,6] have been successfully employed. Among these, CVD has proved to be relatively more effective when aiming for a high yield of single-walled nanotubes. When synthesizing N-doped CNTs by CVD methods, any C/N feedstock requires not only an optimization of the temperature window in which the N-doped nanotubes are formed but also a clear determination of the C−N bonding environments present in the sample,[7–9] which has been shown to be particularly temperature sensitive.[10] Furthermore, the purity of the samples can be compromised not only related to the formation of carbonaceous coproducts but also because of the presence of remaining catalysts. In this context, the possibility of using films of catalytic material has been previously reported[11,12] in order to yield nearly catalyst free nanotubes.

In this work, we report the growth of vertically aligned single- and few-walled N-doped CNTs synthesized by means of CVD of pure acetonitrile on multilayer catalysts of different compositions. The N incorporation profile and morphological characterization have been performed as well as a detailed analysis of the bonding environment according to synthesis parameters. To the best of our knowledge, this method represents the most effective route to producing N-doped few-walled carbon nanotubes free of catalytic material. Concomitant with previous investigations, this provides the advantage that the samples can easily be removed from the catalytic substrate by mild sonication and further employed for applications. In addition, the same substrates can be reused for new synthesis experiments.

* Corresponding author. E-mail: paola@vdg.fis.puc-rio.br.
† Leibniz Institute for Solid State and Materials Research Dresden.
‡ Pontifícia Universidade Católica do Rio de Janeiro.
§ Szczecin University of Technology.

(1) Dresselhaus, M.; Dresselhaus, G.; Avouris, P. *Carbon Nanotubes: Synthesis, Structure, Properties, and Applications*; Springer-Verlag: Germany, 2001.
(2) Terrones, M.; Jorio, A.; Endo, M.; Rao, A.; Kim, Y.; Hayashi, T.; Terrones, H.; Charlier, J.-C.; Dresselhaus, G.; Dresselhaus, M. *Mater. Today* **2004**, 30.
(3) Jr. Hammer, P.; Carvalho, A.; Alvarez, F. *J. Non-Cryst. Solids* **2002**, *299*, 874.
(4) Glerup, M.; Steinmetz, J.; and, D.; Stephan, O.; Enouz, S.; Loiseau, A.; Roth, S.; Bernier, P. *Chem. Phys. Lett.* **2004**, *387*, 193.
(5) Kamalakaran, R.; Terrones, M.; Seeger, R.; Kohler-Redlich, P.; Kim, Y.; Hayashi, T.; Endo, M. *Appl. Phys. Lett.* **2000**, *77*, 3385.
(6) Villalpando-Paez, F.; Zamudio, A.; Elias, A.; Son, H.; Barros, E.; Chou, S.; Kim, Y.; Muramatsu, H.; Hayashi, T.; Kong, J.; Terrones, H.; Dresselhaus, G.; Endo, M.; Terrones, M.; Dresselhaus, M. *Chem. Phys. Lett.* **2006**, *424*, 345.
(7) Bulusheva, L.; Okotrub, A.; Kudashov, A.; Asanov, I. P.; Abrosimov, O. *Eur. Phys. J. D* **2005**, *34*, 271.
(8) Choi, H.; Park, J.; Kim, B. *Jour. Phys. Chem. B* **2005**, *109*, 4333.
(9) Choi, H.; Bae, S.; Park, J.; Seo, K.; Kim, C.; Kim, B.; Song, H.; Shin, H. *Appl. Phys. Lett.* **2004**, *391*, 308.
(10) Ayala, P.; Grüneis, A.; Gemming, T.; Grimm, D.; Kramberger, C.; Rümmeli, M., Jr.; Kuzmany, H.; Pfeiffer, R.; Barreiro, A.; Büchner, B.; Pichler, T. *J. Phys. Chem. C* **2007**, *101*, 2879.
(11) Lacerda, R.; Teh, A.; Yang, M.; Theo, K.; Rupesinghe, N.; Dalal, S.; Koziol, K.; Roy, D.; Amaratunga, G.; Milne, W.; Chowalla, M.; Hasko, D.; Wyczisk, F.; Legagneux, P. *Appl. Phys. Lett.* **2004**, *84*, 269.
(12) Grüneis, A.; Kramberger, C.; Grimm, D.; Gemming, T.; Rümmeli, M.; Barreiro, A.; Ayala, P.; Pichler, T.; Schaman, C.; Kuzmany, H.; Schumann, J.; Büchner, B. *Chem. Phys. Lett.* **2006**, *425*, 301.

10.1021/cm0715592 CCC: $37.00
Published on Web 11/14/2007

Table 1. Different Multilayer Catalytic Substrates Employed

	Si (mm)	SiO_x (μm)	Al_2O_3 (nm)	MgO (nm)	Mo (nm)	Fe (nm)
ML1	0.5	1	10			1
ML2	0.5	1		10		1
ML3	0.5	1		10	0.5	1
ML4	0.5	1	10		1	1

2. Experimental Section

To synthesize the nanotube material, a CVD reactor was built as described in previous work.[13] This experimental setup consists of a quartz tube placed horizontally through a tuneable hot zone tubular furnace. This allows an accurate control of small steps of temperature gradients besides the use of a pumping system, allowing high-vacuum initial conditions. An acetonitrlile C/N feedstock inlet was coupled to a CF type valve on the other end of the furnace to release the solvent.

Pursuing a base growth mechanism, we employed multilayered metallic films of different compositions. The films were deposited on thermally oxidized Si ⟨100⟩ (1μm SiO_x) by means of electron beam evaporation as described in detail elswhere.[12,14] The layer composition and thickness of the multilayered catalyst films are summarized in Table 1.

The multilayers were placed into the CVD reactor, which was subsequently evacuated to a vacuum always better than 1×10^{-7} mbar as base pressure, while the temperature was increased to 200 °C. From this stage, a reduction of the topmost layer was carried out in the presence of a H_2 atmosphere (typically 50 mbar for our system) and evaluated at different temperature values. For the different multilayers, the optimal H_2 treatment temperature was tested independently, increasing the base reduction value of 200 °C with 50 °C steps up to the nanotube growth temperature range (for acetonitrile, from 750 to 900 °C in our experiments). Once this temperature was attained, the system was again evacuated to the initial base pressure and subsequently exposed to the C/N feedstock's vapor. The synthesis time was optimized at 8 min for our system. During this time the pressure in the reactor raised to the value of the vapor pressure of acetonitrile combined with the formed species (a needle valve was employed to maintain ~89 mbar). Immediately after the synthesis, the feedstock was closed and the system was switched off and slowly cooled.

An FEI Nova NanoSEM scanning electron microscope and a FEI Tecnai F30 analytical transmission electron microscope (TEM), operating at 300 keV, were used for an overall morphological characterization. For high-resolution imaging, the nanotube material can easily be detached by mild sonication in isopropanol and transferred onto holey carbon grids. A Bruker FT-Raman spectrometer operating in ambient conditions with a laser excitation of 1.16 eV (1064 nm) was employed. To determine the nitrogen content and the bonding environment within the grown structures, X-ray photoelectron spectroscopy (XPS) was performed using a PHI 5600 spectrometer equipped with a monochromatic Al Kα source (1486.6 eV) operating with a base pressure of 1×10^{-9} mbar and an overall spectral resolution of 0.5 eV. To map the surfaces of the catalysts, we used a multimode AFM (Nanoscope IIIa, Digital Instruments) equipped with a Si_3N_4 tip ($K = 0.075$ N/m). The microscope was operated in contact mode for checking the surface. The images presented here have been treated by a simple planar processing.

(13) Grimm, D.; Grüneis, A.; Kramberger, C.; Rümmeli, M.; Barreiro, A.; Pichler, T.; Kuzmany, H.; Büchner, B. *Chem. Phys. Lett.* **2006**, *428*, 416.

(14) Delzeit, L.; Chen, B.; Cassell, A.; Stevens, R.; Nguyen, C.; Meyyappan, M. *Chem. Phys. Lett.* **2001**, *348*, 368.

3. Results and Discussion

The structure of the multilayered substrate has been observed to play a crucial role in the material growth. As illustrated in Table 1, four different layer combinations (from this point labeled in the text as ML1−ML4) were employed. These have been previously shown to be efficient for vertically aligned SWCNT growth from cyclohexane.[12] In that case, the composition from ML1 was optimal. However, the nanotube yield achieved with ML1 when using acetonitrile is relatively small. In this case, the catalyst films containing MgO (ML2−ML4) worked better. The highest yield was optimized employing the ML2 composition. This film, in contrast to ML3 and ML4, contains no Mo as cocatalyst. Unless stated differently, ML2 was used for the optimization of the acetonitrile-based growth of N-doped vertically aligned CNTs.

To analyze the superficial morphology of these catalysts' prior nanotube growth, we inspected the substrates with and without H_2 treatment by AFM and SEM. To visualize the superficial changes according to the pretreatment, we show a summary of representative images in Figure 1. Starting with the substrates annealed without H_2 shown in the right lower panel in Figure 1d, we can observe the profile of three substrates that were heated to 800 (d_2), 500 (d_3), and 300 °C (d_4) in vacuum. The SEM image in Figure $1d_1$ represents the typical top view of a substrate after heating. No evident difference was observed between surfaces by this method; therefore, a further AFM analysis was required in order to visualize the detailed superficial structure. The corresponding images are shown in the same 1d panel and their roughness (rms) values are 51.96, 29.431, and 31.37 nm, respectively. As clearly noticed, the higher temperature produces a higher roughness of the surface, which can be attributed to the decomposition (oxygen liberation from the second-layer MgO) or detachment due to superficial tension.

Looking at the images obtained from the same catalytic multilayer film but now with H_2 treatment, we clearly see that the surface morphology is not only influenced by the temperature but also by the presence of hydrogen. The roughness of the surface suffers an evident transformation that favors the formation of nanometer-scale islands on the films that appear retracted because of the heating treatment. Images a−c in Figure 1 correspond to the H_2 treatment starting at 500, 350, and 300 °C, respectively. It is also observed that the increase in the temperature produces higher roughness of the surface. However, the local morphology varies by the temperature at which the H_2 treatment is applied. The apparent porosity of the topmost layer upon treatment exhibits a favorable catalytic activity toward the synthesis of SWNTs, and this leads us to pay special attention to the pretreatment of the catalysts, which is analyzed in detail in the following paragraphs.

It has been observed that their activation through H_2 reduction has a crucial effect on the formation of nanotubes. Not only the morphology and yield are affected but also the nitrogen incorporation profile. If no reduction at all is employed, very limited nanotube growth is observed. The same situation occurs when starting the reduction above 750 °C. We have observed that the ideal temperature window at

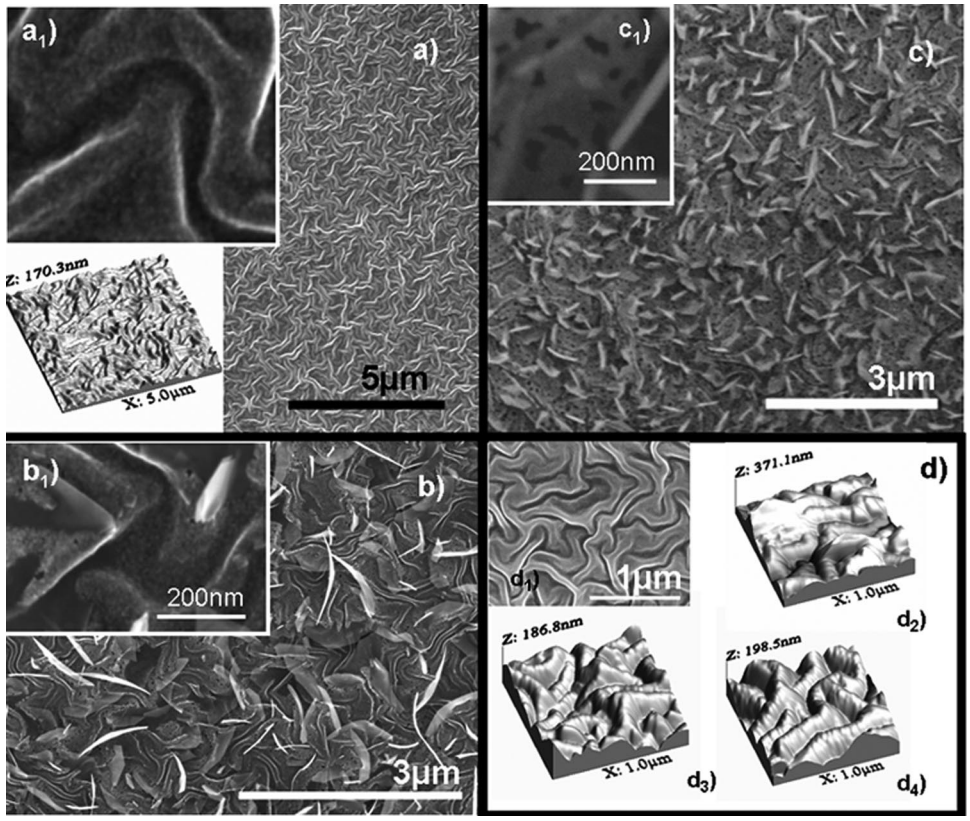

Figure 1. AFM and SEM superficial characterization of a multilayer substrate of 10 nm MgO and 1 nm Fe after annealing at (a−c) 800, 500, and 300 °C, respectively, in the presence hydrogen, and (d) in a vacuum.

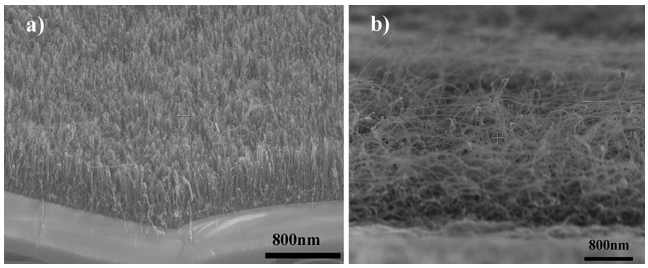

Figure 2. SEM characterization of nanotubes grown from acetonitrile employing multilayered catalytic films. (a) Micrograph exhibiting the overall morphology of vertically aligned N-doped nanotubes in a sample grown from a catalytic film reduced at 200 °C. (b) High-magnification micrograph of nanotube material grown from a multilayer without H_2 treatment.

which the films should be reduced is between 250 and 500 °C for optimal yield. Out of this range, the nanotube growth amount decreases dramatically either because of the formation of superficial compounds attached to the topmost layer inhibiting the catalytic activity or rapid aggregation of the thin Fe layer.[15,16] Furthermore, the optimal temperature window in which few-walled nanotube material is formed lies between 790 and 880 °C, independent of the H_2 treatment. In Figure 2a wide-area SEM micrograph shows vertically aligned nanotubes with uniform lengths of $\sim 5\ \mu$m over an area of 1 mm^2. The substrates that had no H_2 reduction exhibited a much lower yield characterized by spaghetti-like structures laying on the substrate surface as seen in Figure 2b. Unlike the supported and floating catalyst CVD methods, using multilayer catalysts for the production of N-doped nanotubes increases the width of the temperature window in which N-doped few-walled nanotubes are grown effectively with substitutional doping. This will be discussed on the XPS analysis later in this section. The catalytic activity of the film has to be optimized in direct relation with the feedstock. Even when using pure C/N feedstocks widely employed for N-doped nanotube growth, such as benzylamine and acetonitrile, we obtain completely different results. Just for comparison purposes, we tested the same multilayered film in a benzylamine environment, which has proved to yield high-quality N-doped nanotubes by different synthesis methods.[6,10] A sample grown from the ML2 film with a acetonitrile C/N source yields a dense growth of vertically aligned few-walled nanotubes, whereas the same multilayered substrate in a benzylamine environment exhibits a 10:1 decrease in nanotube formation. In addition, it has been observed that the reduction process has a direct influence on the N incorporation within the nanotube structure, where the bonding environments formed are strongly dependent on this pretreatment.

The samples that exhibited dense forests of vertically aligned nanotubes were removed from the substrate and dispersed in isopropanol to be examined by means of bright-field and high-resolution TEM (see Figure 3a−h). It has been corroborated that this method effectively yields practically catalyst free samples. Furthermore, employing acetonitrile

(15) Rümmeli, M.; Borowiak-Palen, E.; Gemming, T.; Pichler, T.; Knupfer, M.; Kalbác, M.; Dunsch, L.; Jost, O.; Silva, S.; Pompe, W.; Büchner, B. *Nano Lett.* **2005**, *5*, 1209.
(16) Baker, R.; Alonzo, J.; Dumesic, J.; Yates, D. J. *Catalysis* **1982**, *77*, 74.

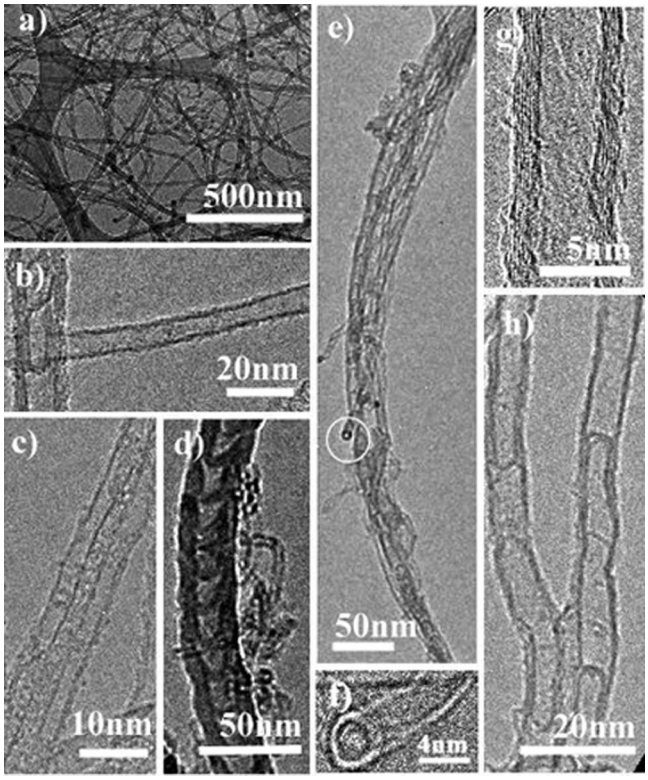

Figure 3. Transmission electron microscopy characterization of nanotubes grown from acetonitrile employing multilayered catalytic films. (a) Low-magnification micrograph showing the overall morphology of a vertically aligned sample removed from the substrate by mild sonication. (b) Multiple morphology sample exhibiting a thin nanotube and part of a compartmentalized N-containing nanotube. (c) Bundled N-doped SWNTs. (d, e) Single- and double-walled nanotubes rolled around and bundled with MWNTs. The high-magnification image in (f) corresponds to the circled area in Figure e. (g) High-resolution image of a MWNT with 8 walls and hollow-core. This morphology predominates in samples grown between 790 and 880 °C. (h) Few-walled nanotubes with compartmentalized structure.

as feedstock, we obtained N-doped few-walled nanotubes in the optimal temperature and pretreated catalyst conditions. Regarding the morphology of individual tubes,we observed that for the highest yield of vertically aligned samples, the nanotube films are up to 5 μm long. However, a less densely packed growth leads to the formation of tubes that can be longer (more than 3 times longer). As described later in detail, a multiple morphology with predominating SWNTs (images b and c in Figure 3) and few-walled nanotubes (Figure 3e−h) is obtained in optimal conditions. We observed in all samples that although the number of walls does not exceed eight shells (Figure 3g) under the same circumstances, the morphology of compartmentalized nanotubes is unavoidable when employing acetonitrile. A bamboolike structure is characteristically observed in most N-containing nanotubes,[3,4,17,18] forming stacked pockets in which nitrogen encapsulates. In our samples, a low percentage of thick bamboo-like MWNTs (see Figure 3d) has been found (<20%). In these few formed MW tubes, in contrast to previously reported work,[18] we have not observed an increase in the diameter of multiwalled tubes according to the temperature. The predominant morphology in all samples in the 790 and 880 °C window corresponds to single- and few-walled N-doped nanotubes. For the samples grown in this temperature window, in which the substrate was reduced starting from 250 °C, ∼50% of the nanotubes have up to 4 walls and exhibit compartmentalized structure, in which the sections range between 20 and 40 nm in the direction along the tube axis as illustrated in Figure 3h.

The micrograph shown in figure 3a is a low-magnification overall view of a sample grown from a substrate reduced at 500 °C. From an image evaluation, we observe that in this case, the presence of thick multiwalled nanotubes (>8 walls) is more evident. Nevertheless, in these samples, single- and double-walled nanotubes are also present and appear attached or rolled around the long thick MWNTs (Figure 3d) and bundled with thin few-walled nanotubes (Figure 3e). The high-magnification image in Figure 2f corresponds to the circled area in Figure 3e that shows a cross-section of an opened DWNT. For the optimal conditions with the highest yield of few layer CNTs (T = 835 °C, H_2 treatment between 250 and 500 °C, ML2) we performed a statistical analysis of several TEM micrographs and observed a diameter distribution between 1 and 5 nm with a maximum around 2 nm. This distribution of the small nanotubes is independent of the synthesis temperature and H_2 treatment, but strongly depends on the type of the multilayer catalyst. The actual difference lies in the overall yield of these N-doped nanotubes.

In summary, it is important to notice that the catalytic substrate reduction plays a crucial role in the structure of the nanotubes. Furthermore, it has been observed that the bonding environment of the N in the doped structures varies dramatically according to the reduction of the uppermost oxidized layer. To elucidate the influence of the two key synthesis parameters on the high yield growth of thin CNTs (the synthesis temperature and H_2 treatment for efficient catalyst reduction), we performed a detailed study of the nanotube growth from ML2 films. Therefore, we analyzed in detail the bulk properties of tubes grown from ML2 films reduced at 300 and 500 °C.

We now turn to a detailed Raman analysis of the overall yield of small nanotubes and the overall defect concentration. The results for the films reduced at 300 and 500 °C are depicted in Figures 4 and 5, respectively. The left panels of the figures show the radial breathing modes (RBM) of thin nanotubes. It is well-known that the diameters of thin tubes can be determined by $\omega_{RBM} = 223/d_t + 10$.[19] With the 1064 nm laser from the FT-Raman spectrometer, the RBM mode responses between 225 and 300 cm^{-1}, corresponding to SWNT diameters between 0.6 and 1.2 nm, are visible in both cases. This outlines the efficiency of pure acetonitrile as a C/N feedstock to produce high-quality SWNTs. The highest relative yield of these nanotubes is peaked around 835 °C. It is worth noting that for the two sets of samples, the synthesis temperature window is remarkably different. When the

(17) Reyes-Reyes, M.; Grobert, N.; Kamalakaran, R.; Seeger, T.; Golberg, D.; Rühle, M.; Bando, Y.; Terrones, M.; Terrones, M. *Chem. Phys. Lett.* **2004**, *396*, 167.
(18) Lee, Y.; Kim, N.; Bae, S.; Park, J.; Yu, S.; Ryu, H.; Lee, H. *J. Phys. Chem. B* **2003**, *107*, 12958.
(19) Fantini, C.; Jorio, A.; Souza, M.; Dresselhaus, M.; Pimenta, M. *Phys. Rev. Lett.* **2004**, *93*, 147406.

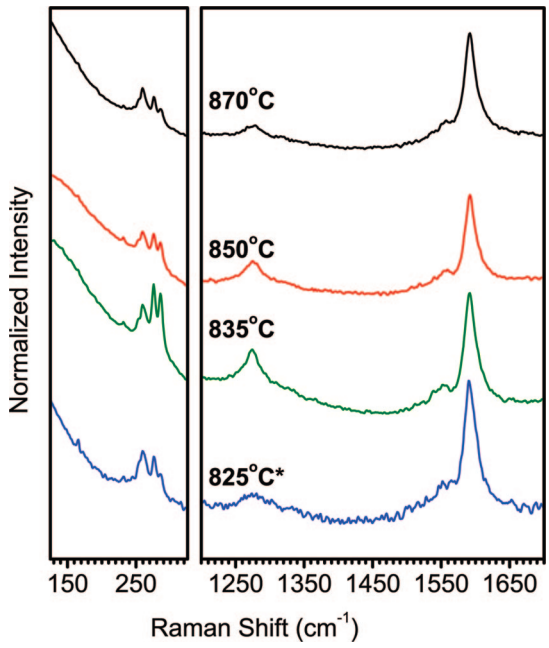

Figure 4. Raman spectra of a sample synthesized with H_2 reduction at 300 °C. The left side panel shows the RBM corresponding to the single-walled nanotubes present in the sample. The right side shows the relative D/G ratio. The (*) 825 °C represents a sample grown in the furnace zone where the feedstock has not reached the maximum temperature.

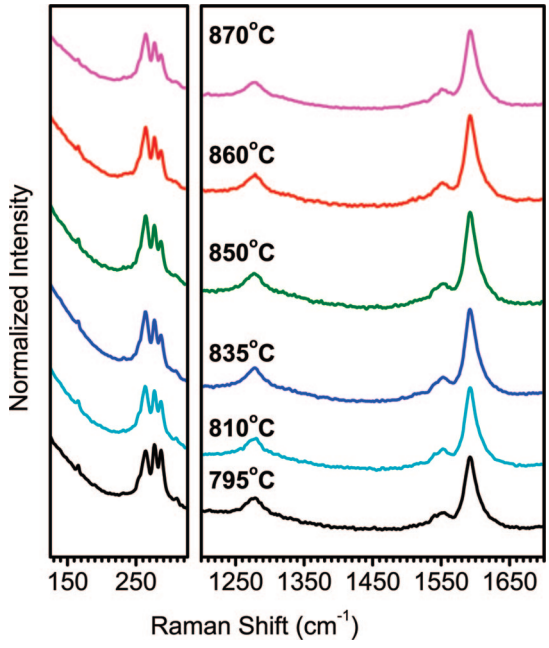

Figure 5. Raman spectra of a sample synthesized with H_2 reduction at 500 °C. The RBM correspond to the laser resonance single-walled nanotubes present in the sample. The right side shows the relative D/G ratio.

substrate is reduced at 300 °C, the yield drops noticeably with temperature, whereas for the 500 °C treatment, a low variation of the yield is observed with the synthesis temperature. In addition, the thicker nanotubes observed in our TEM analysis for both sets of samples are outside the resonance window of our FT-Raman system. The right panel depicts the disorder-induced second-order defect D-line and the tangential modes (G-lines), respectively. From the intensity ratio of the D and G lines, the relative defect concentration can be evaluated. For CVD-grown

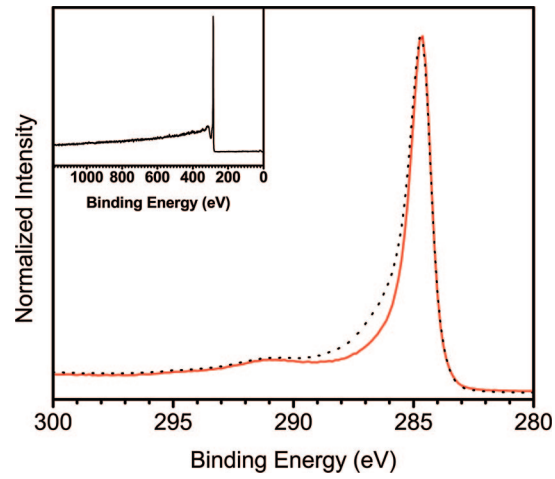

Figure 6. Typical C1s spectra of the samples synthesized from the different multilayered samples. The red solid curve corresponds to the sample reduced at 500 °C, the dotted black line is the sample reduced at 300 °C, respectively. The inset shows a typical survey scan of the samples.

MWCNT, this value usually ranges between 1:1 and 1:2,[20] revealing a high defect concentration. On the other hand, for SWNT and double-walled NT, the D/G ratio is much lower and on the order of 1:20 for both pristine[21] and N-doped samples.[10] We observed that the optimal D/G ratio is 1:15. The relative defect concentration is also related to the overall yield of thin nanotubes. This illustrates a strong influence of the synthesis window on the quality of the nanotube material produced.

As a final point we turn to the analysis of the elemental composition of the as-produced samples by means of XPS in order to detect the content and bonding environment of the carbon and N species. Figure 6 depicts a comparison of the C1s spectra obtained for the two sets of samples. It turned out that for both sets, the position and line shape of the C1s response is independent from the synthesis temperature. Therefore, each curve represents a typical spectrum with the main peak at 284.7 eV. This value is similar to the previously reported for pristine and N-doped SWNT and DWNT[10,22] and confirms the nearly pure formation of carbon nanotubes employing acetonitrile as feedstock. The actual difference between the corresponding C1s peaks of the two sets lies in the line shape. Pristine samples, as well as N-doped samples with low doping, show a Doniach−Sunjic line shape with a small asymmetry. In our samples, a pronounced shoulder at 287 eV is observed. This shoulder is attributed to a distribution of different C−N bonding species. From the relative intensities between the overall C1s to the overall N1s response and taking into account the relative atomic cross sections, we observe a N content of 2% for the samples reduced at 500 °C and 6% for the samples reduced at 300 °C. In both cases, this overall N content is only weakly

(20) Barreiro, A.; Kramberger, C.; Rümmeli, M.; Grüneis, A.; Grimm, D.; Hampel, S.; Gemming, T.; Büchner, B.; Bachtold, A.; Pichler, T. *Carbon* **2006**, *45*, 55.
(21) Grüneis, A.; Rümmeli, M.; Kramberger, C.; Barreiro, A.; Pfeiffer, R.; Kuzmany, H.; Gemming, T.; Pichler, T.; Büchner, B. *Carbon* **2006**, *44*, 3177.
(22) Kramberger, C.; Rauf, H.; Shiozawa, H.; Knupfer, M.; Büchner, B.; Pichler, T. *Phys. Rev. B* **2007**, *75*, 235437.

dependent on the synthesis temperature. This is in good agreement with the above-mentioned interpretation of C−N bonding species, because the shoulder in the C1s response is much more pronounced in the latter having roughly double the relative intensity.

To gain more insight into the bonding environment of the different N species and the N incorporation profile in the produced nanotubes,we performed a detailed line shape analysis of the two sets of samples. For the nitrogen spectra recorded in the ntrogen region as depicted in Figure 7, we observe that the N incorporation profile for both sets of samples varies drastically from one to another. However, we observe in all of them that the spectral decomposition gives a defined relative percentage of sp^2 substitutional configuration, pyridinic configuration, and gaseous components mainly related to volatile compounds containing C−H−N.[23] The spectra used for deconvolution are in good agreement with previous results reported for N-doped CNTs,[7–10,24,25] even though, at the present research stage, there is still somehow divergence in accurately assigning the peaks corresponding to the different bonding environments. This is mostly related to the one-dimensional nature of carbon nanotubes in comparison with other nitrogen-containing carbon systems. In the top panel in Figure 7, the spectra used for deconvolution are centered in 398.6, 400, 400.88, 402, and 404 eV, whereas the spectra below, used for the second set deconvolution, correspond to the same values plus an extra peak at 405.1 eV that has been assigned to molecular N_2 intercalated within the walls of the nanotubes.[9] The peaks centered at 398.6 and 400.88 eV correspond to the pyridine and substitutional N incorporation, whereas the 402 and 404 eV signals are attributed to oxidic species or N physisorbed on graphite.[8] The 400 eV response has been reported for compounds containing C, H, and N; however, we cannot rule out the fact that it could also correspond to response of the substitutional configuration because of structural effects.

With this interpretation, for the samples synthesized after reduction at 300 °C, it has been observed that the maximum N content present in the samples is ∼6%, exhibiting a higher component of sp^2 configuration with a ratio of about 1:2 to the pyridinic structure. The gaseous N components are below 10%. Interestingly, the component of the substitutional sp^2 structures is strongly dependent on the synthesis temperature. For the samples synthesized from multilayers reduced at 500 °C, the story changes. The observed N content is ∼2%. In this case, the ratio between the sp^2, pyridinic, and incorporated N-gaseous species is roughly 1:1:1 and only slightly temperature-dependent (bottom panel in Figure 7). This fact highlights that the sp^2 configuration competes with the formation of pyridinic species and the incorporation of N gaseous species. The actual maximal substitutional doping of the nanotubes in the optimal conditions for the two different sets of samples represents about ∼1/2 and ∼1/3 of the total N content. respectively.

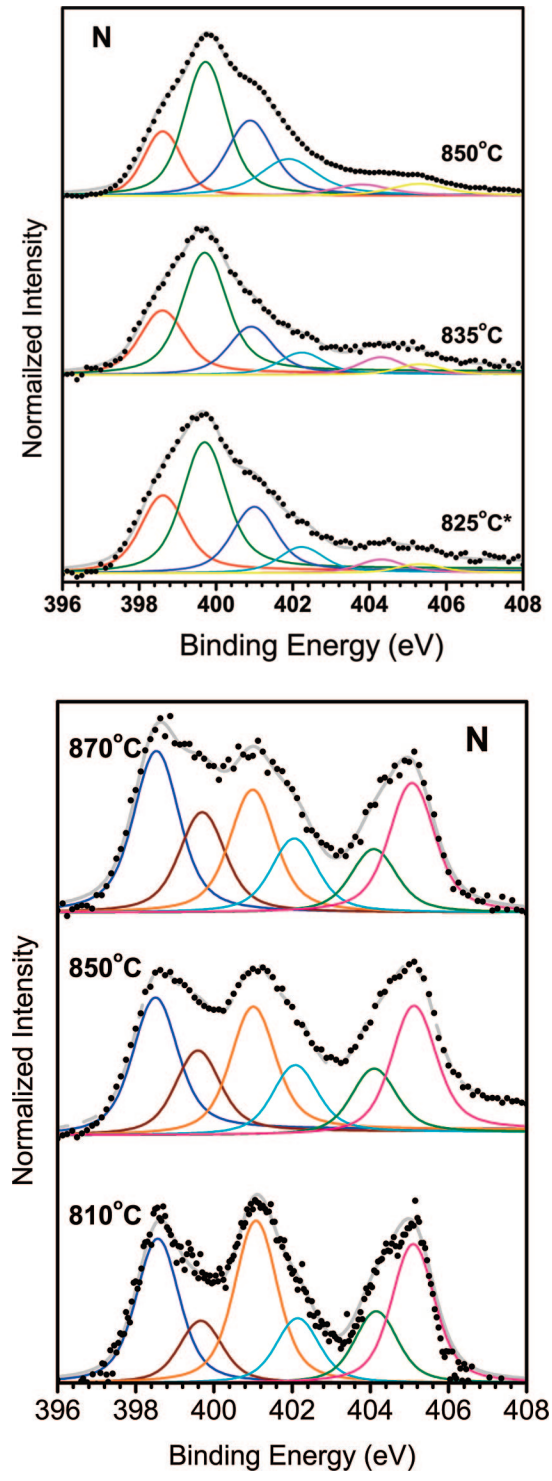

Figure 7. XPS spectra corresponding to the N1s core level from multilayers reduced at 300 (upper panel) and 500 °C (lower panel), respectively. The collected data are represented in dots, whereas the thin solid line depicts the results of the fitted spectra. The deconvolution of the N1 response has been made with six peaks generated from the different N bonding environments, which in both cases include the pyridinic (398.6 eV) and substitutional configuration (400.6−400.88 eV).

The maximum N content remains constant through the synthesis; however, the N incorporation profile varies within a temperature window determined by the catalyst activity tunable through its pretreatment. This is in good agreement with previous studies on SW and DW N-doped nanotubes.[10,25]

(23) Johansson, A.; Strafström, S. *J. Chem. Phys.* **1999**, *111*, 7.
(24) Choi, H.; Bae, S.; Jang, W.-S.; Jung, H.; Park, J.; Song, H.; Shin, H.-J.; Ahn, J.-P. *J. Phys. Chem. B* **2005**, *109*, 1683.
(25) Kim, S.; Lee, J.; Na, C.; Park, J.; Seo, K.; Kim, B. *Chem. Phys. Lett.* **2005**, *413*, 300.

4. Conclusions

Vertically aligned thin N-doped nanotubes with a tuneable and defined doping level have been synthesized employing CVD with multilayered catalysts and a pure acetonitrile C/N feedstock. It has been observed that the catalytic substrate reduction plays a critical role in the yield and the structure of the nanotubes. The synthesis temperature and the temperature of the catalyst reduction by H_2 are crucial. In the ideal synthesis temperature window, the predominant morphology consists of SW, DW, and few-walled NTs with compartments between 20 and 40 nm along the tube axis. Depending on the process parameters, we are able to tune the nitrogen content and the formation ratio of small N-doped nanotubes to bamboo nanotubes.

Acknowledgment. We acknowledge the financial support of the following agencies and projects: The Brazilian Agencies CNPq and FAPERJ, DAAD (Probral D/04/40433) and DFG for projects PI 440/3. A.G. acknowledges an individual Marie Curie fellowship from the European Union (EU). MHR acknowledges the EU (CARBIO project).

CM0715592